A&A 374, 412–420 (2001)
DOI: 10.1051/0004-6361:20010732

Astronomy & Astrophysics

Oxygen abundances in dwarf irregular galaxies and the metallicity–luminosity relationship

L. S. Pilyugin*

Main Astronomical Observatory of National Academy of Sciences of Ukraine, Goloseevo, 03680 Kiev-127, Ukraine

Received 20 December 2000 / Accepted 2 May 2001

Abstract. The low-luminosity dwarf irregular galaxies are considered. The oxygen abundances in H II regions of dwarf irregular galaxies were recalculated from published spectra through the recently suggested P–method. It has been found that the metallicity of low-luminosity dwarf irregular galaxies, with a few exceptions, correlates well with galaxy luminosity. The dispersion of oxygen abundances around the metallicity–luminosity relationship increases with decreasing galaxy luminosity, as was found by Richer & McCall (1995). The absence of a relationship between the oxygen abundance and the absolute magnitude in the blue band for irregular galaxies obtained by Hidalgo-Gámez & Olofsson (1998) can be explained by the large uncertainties in the oxygen abundances derived through the T_e–method, that in turn can be explained by the large uncertainties in the measurements of the strengths of the weak oxygen line [OIII]λ4363 used in the T_e–method.

Key words. galaxies: abundances – galaxies: ISM – galaxies: irregular – galaxies: individual: NGC 6822

1. Introduction

Twenty years ago Lequeux et al. (1979) revealed that the oxygen abundance correlates with total galaxy mass for irregular galaxies, in the sense that the higher the total mass, the higher the heavy element content. Since the galaxy mass is a poorly known parameter, the metallicity–luminosity relation instead of the mass–metallicity relation is usually considered (Skillman et al. 1989a; Richer & McCall 1995; Hidalgo-Gámez & Olofsson 1998; Hunter & Hoffman 2000; Pilyugin & Ferrini 2000b; among others). It has been found that the characteristic gas-phase abundances (the oxygen abundance at a predetermined galactocentric distance) and luminosities of spiral galaxies are also correlated (Garnett & Shields 1987; Vila-Costas & Edmunds 1992; Zaritsky et al. 1994; Garnett et al. 1997), and this relationship maps almost directly on to the metallicity–luminosity relationship of irregular galaxies (Zaritsky et al. 1994; Garnett et al. 1997).

Richer & McCall (1995) have revealed a prominent feature of their metallicity–luminosity relation for irregular galaxies: they have found more scatter at low luminosities, though they found less at high luminosities. The onset of this scatter seems to occur at $M_B \sim -15$ or $\log L_B \sim 8.2$. Moreover, Hidalgo-Gámez & Olofsson (1998) have found that there is no relationship between the oxygen abundance and the absolute magnitude in the blue band for dwarf irregular galaxies ($M_B > -17$ or $\log L_B < 9$). Hunter & Hoffman (2000) have found that their samples do generally cluster around the relationship between M_B and O/H derived by Richer & McCall (1995) but do not themselves define a linear relationship very well, appearing more as a cloud of points with a large scatter around the line. In particular, the scatter becomes larger for $M_B > -16$. Hunter & Hoffman (2000) have concluded that the relationship between O/H and M_B is very general over the Hubble sequence but the scatter is very large and discerning the trend over a limited parameter range is hard. They noted that perhaps the interesting science lies in this scatter, although a part of this scatter is undoubtedly due to the uncertainties in determining O/H and M_B.

The most precise method of determining the abundances of H II regions requires the detection of [OIII]λ4363 emission line (the T_e–method). The [OIII]λ4363 emission line appears in high excitation spectra of oxygen-poor H II regions and is usually undetectable in spectra of oxygen-rich H II regions. Then, in the general case, the precision of the oxygen abundance determination in oxygen-poor H II regions is higher than in oxygen-rich H II regions. The derived oxygen abundances of metal-poor H II regions in blue compact galaxies possessing very bright emission lines are accurate to within 0.05 dex (Izotov & Thuan 1999). However, many irregular galaxies have no bright H II regions with readily measured emission lines. As was noted by Hidalgo-Gámez & Olofsson (1998) the

* e-mail: pilyugin@mao.kiev.ua

uncertainties in the intensity of the line [OIII]λ4363 in spectra of H II regions in dwarf irregular galaxies reported in the literature fluctuate between 11% and 120%. Thus, in reality, the precision of oxygen abundance determination in dwarf irregular galaxies seems to be rather low.

In our recent work (Pilyugin 2000 Paper I, 2001 Paper II) a new method for oxygen abundance determination in H II regions (the P–method) has been constructed, starting from the idea of McGaugh (1991) that the strong oxygen lines ([OII]$\lambda\lambda$3727, 3729 and [OIII]$\lambda\lambda$4959, 5007) contain the necessary information for determination of accurate abundances in H II regions. By comparing oxygen abundances in bright H II regions derived (with high precision) through the T_e–method, O/H_{T_e}, and those derived through the suggested P–method, O/H_P, it has been found that the precision of oxygen abundance determination with the P–method is comparable to that of the T_e–method. Then it can be expected that in faint H II regions, in which the temperature-sensitive line [OIII]λ4363 is measured with large uncertainty, the P–method provides more realistic oxygen abundances than the T_e–method since only the strong (and as a consequence, more readily measurable) oxygen lines are used in the P–method. Moreover, the P–method is workable in the cases when the temperature-sensitive line [OIII]λ4363 is undetectable. Thus, we can expect that the application of the P–method to the oxygen abundance determination in faint H II regions of dwarf irregular galaxies allows us to refine the oxygen abundances in H II regions with low-precision measurements of line [OIII]λ4363 and to determine the realistic oxygen abundances in H II regions with undetectable line [OIII]λ4363. We hope that it can clarify whether the luminosity–metallicity relationship for irregular galaxies still persists or disappears at the low-luminosity end. This is a goal of the present study.

2. The $Z-L$ relationship of low-luminosity irregular galaxies

2.1. The preliminary remarks

The relation of the type $O/H = f(P, R_3)$ between oxygen abundance and the values of P and R_3 has been derived empirically in Papers I and II using the available oxygen abundances determined via measurement of the temperature-sensitive line ratio [OIII]4959, 5007/[OIII]4363. Notations similar to those in Papers I and II will be adopted here: $R_2 = I_{[OII]\lambda3727+\lambda3729}/I_{H\beta}$, $R_3 = I_{[OIII]\lambda4959+\lambda5007}/I_{H\beta}$, $R = I_{[OIII]\lambda4363}/I_{H\beta}$, $R_{23} = R_2 + R_3$, $X_{23} = \log R_{23}$, and $P = R_3/R_{23}$. The excitation index P used in Paper II and indexes p_2 and p_3 used in Paper I are related through simple expressions: $p_3 = \log P$ and $p_2 = \log(1 - P)$. The following equations for the oxygen abundance determination in low-metallicity H II regions have been suggested in Paper I

$$X_3^* = X_3^{obs} - 2.20\, p_3, \quad (1)$$

and

$$12 + \log(O/H)_P = 6.35 + 1.45\, X_3^*. \quad (2)$$

Equations (1) and (2) can be rewritten as

$$12 + \log(O/H)_P = 6.35 + 1.45\, \log R_3 - 3.19\, \log P. \quad (3)$$

Equation (3) shows that the positions in the R_3–P diagram can be calibrated in terms of oxygen abundance (Fig. 1).

The relationship between oxygen abundance and strong line intensities is double valued with two distinctive parts named usually as the lower and upper branches of the R_{23}–O/H diagram, and so one has to know in advance on which branch of the R_{23}–O/H diagram the H II region lies. The above expression for the oxygen abundance determination in H II regions, Eq. (3), is valid for H II regions with 12 + log(O/H) less than around 8 (Paper I). According to the metallicity–luminosity relationship for irregular galaxies after Richer & McCall (1995), the oxygen abundances in the low-luminosity irregular galaxies ($M_B > -15 \div -16$) are expected to lie in this range. Then it has been adopted here that the H II regions in the low-luminosity irregular galaxies ($M_B > -15 \div -16$) lie on the lower branch of the R_{23}–O/H diagram. Furthermore, only the high-excition ($P > 0.5$) H II regions will be considered here because Eqs. (1) and (2) (linear approximation) have been derived based on the high-excition H II regions.

2.2. Hidalgo-Gámez & Olofsson sample

Firstly the Hidalgo-Gámez & Olofsson (1998) sample of irregular galaxies will be considered. The $R_3 - P$ diagram for H II regions with $M_B > -16$ from Hidalgo-Gámez & Oloffson (1998) sample is shown in the Fig. 1 (panel *a*). The squares are H II regions with 12+log O/H < 7.4, the pluses are those with 7.4 ≤ 12+log O/H < 7.6, the triangles are those with 7.6 ≤ 12+log O/H < 7.8, the crosses are those with 7.8 ≤ 12+log O/H < 8.0, and the circles are those with 12+log O/H ≥ 8.0. The dashed curves are the R_3–P relations obtained from Eq. (3) for fixed values of O/H. Each curve is labeled with the corresponding value of 12+log O/H. For comparison the R_3–P diagram for "calibrating H II regions" from Paper I is also shown in Fig. 1 (panel *b*). Examination of Fig. 1 (panel *a*) shows that the oxygen abundances O/H_{T_e} derived through the classical T_e–method are in conflict with the oxygen abundances corresponding to their positions in the R_3–P for a number of H II regions from the Hidalgo-Gámez & Olofsson (1998) sample of irregular galaxies. It can be explained by the large uncertainties in the oxygen abundances derived through the T_e–method, that in turn can be explained by the large uncertainties in the measurements of the strengths of the weak oxygen line [OIII]λ4363 used in the T_e–method.

The oxygen abundances in H II regions of low-luminosity ($M_B > -16$) irregular galaxies have been recalculated through the P–method. The intensities of

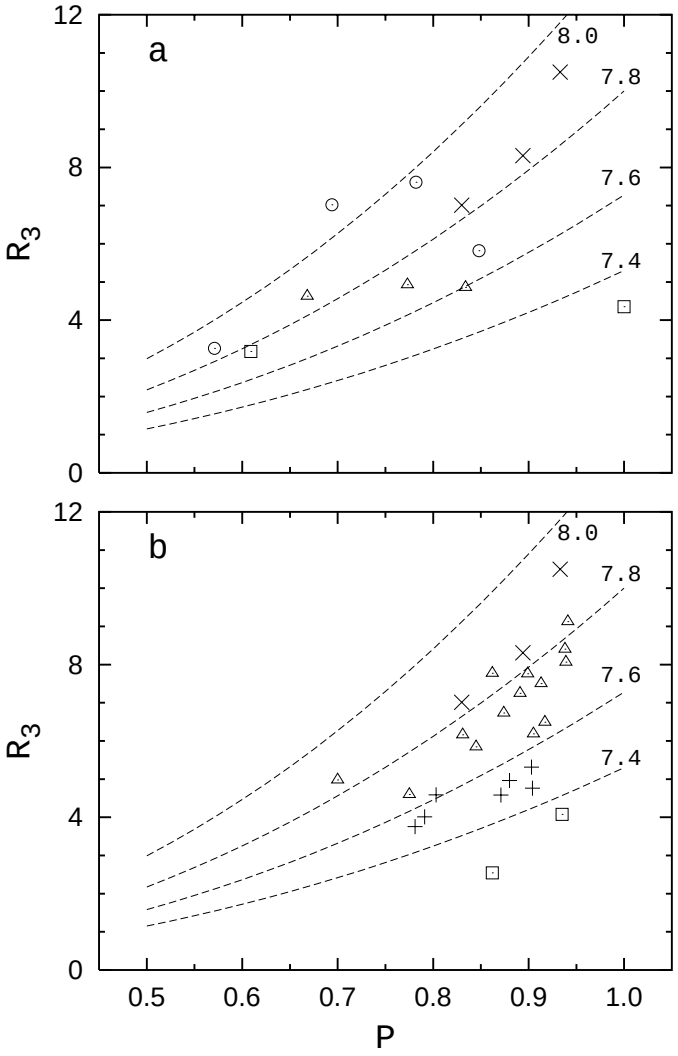

Fig. 1. The R_3–P diagram for H II regions with $M_B > -16$ from Hidalgo-Gámez & Oloffson (1998) sample (panel *a*) and for "calibrating H II regions" from Paper I (panel *b*). The squares are H II regions with 12+log O/H < 7.4, the pluses are those with 7.4 ≤ 12+log O/H < 7.6, the triangles are those with 7.6 ≤ 12+log O/H < 7.8, the crosses are those with 7.8 ≤ 12+log O/H < 8.0, and the circles are those with 12+log O/H ≥ 8.0. The dashed curves are R_3–P relations predicted by the calibration for fixed values of O/H. Each curve is labeled with the corresponding value of 12+log O/H.

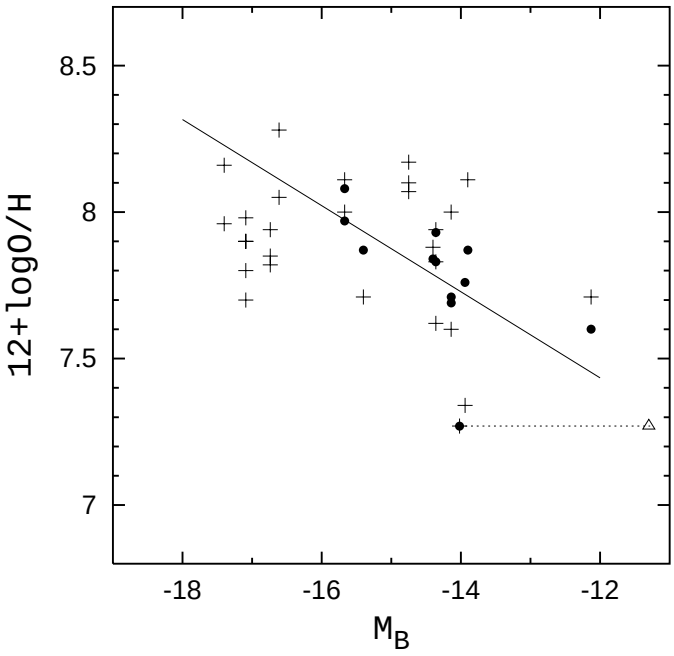

Fig. 2. The metallicity–luminosity diagram for dwarf irregular galaxies. The metallicity–luminosity diagram after Hidalgo-Gámez & Olofsson (1998) based on the oxygen abundances determined with the T_e–method is presented by the pluses. The metallicity–luminosity diagram based on the oxygen abundances derived with the P–method is shown by the filled circles. The positions of Leo A with luminosity from Hidalgo-Gámez & Olofsson and with luminosity adopted here (triangle) are connected with dashed line. The solid line is the L–Z relationship after Richer & McCall (1995).

[OII]$\lambda\lambda$3727, 3729 and [OIII]$\lambda\lambda$4959, 5007 lines were taken from the sources cited by Hidalgo-Gámez & Olofsson (1998): Skillman et al. (1989) (DDO 47, Leo A, Sext A); Moles et al. (1990) (Sext B, GR 8); González-Riestra et al. (1988) (Mkn 178); Heydari-Malayeri et al. (1990) (IC 4662); Webster et al. (1983) (IC 5152); Hodge & Miller (1995) (WLM). The NGC 6822 is excluded from consideration here, this galaxy will be discussed below. The oxygen abundances have been recalculated with the P–method in 12 H II regions of 9 dwarf irregular galaxies. The H II regions A1 and A2 in IC 4662 have oxygen abundances 12+log O/H$_P$ = 7.97 and 8.08, respectively. These H II regions seems to belong to the transition zone of the R_{23}–O/H diagram, and in the strict sense Eq. (3) cannot be used for oxygen abundance determination in these H II regions since Eq. (3) was derived for H II regions with 12+log O/H ≤ 7.95 (the lower branch of the R_{23}–O/H diagram). The metallicity–luminosity diagram for dwarf irregular galaxies from Hidalgo-Gámez & Olofsson (1998) is represented in Fig. 2 by the pluses. The metallicity–luminosity diagram for dwarf irregular galaxies with $M_B > -16$ with the oxygen abundances recalculated through Eq. (3) is shown in Fig. 2 by the filled circles. In order to clearly recognize the influence of the oxygen abundance redetermination on the metallicity–luminosity diagram, the same values of M_B as in Hidalgo-Gámez & Olofsson were used.

It can be easily seen in Fig. 2 that the metallicity–luminosity relation for dwarf irregular galaxies based on the oxygen abundances derived with the P–method shows appreciably less scatter than that based on the oxygen abundances derived with the T_e–method. It is strong evidence in favor of the large scatter in the low-luminosity end of the metallicity– luminosity relation for irregular galaxies being explained mainly by the uncertainty in oxygen abundance determination with the T_e–method.

It should be noted that the abundances used by Hidalgo-Gámez & Olofsson were not taken directly from the sources listed but have been recalculated in a

consistent way and as a consequence the differences in techniques and atomic data do not contribute to the scatter. Then, the increased scatter in oxygen abundances derived with the T_e–method, compared to the scatter in oxygen abundances derived with the P–method seems to be explained by the observational uncertainties in the [OIII]λ4363 line strengths.

A well defined trend is seen between M_B and O/H_P, Fig. 2. The deviations of O/H_P from a linear relationship for all, with one exception, of the H II regions are within $\pm$0.1 dex. The point with a large deviation (in excess of 0.4 dex) corresponds to the dwarf galaxy Leo A. The H II region observed in Leo A is a planetary nebula with no detectable [OII]$\lambda\lambda$3727, 3729 lines; $P = 1$ was adopted in the oxygen abundance determination through the P–method. It cannot be excluded that the P–method calibrated on the basis of H II regions is inapplicable in the case of planetary nebulae. It should be noted, however, that the oxygen abundance in Leo A derived with the P–method agrees remarkably with the oxygen abundance derived by Skilman, et al. (1989). The deviation of Leo A from the relationship seems to be caused by the uncertainty in the integrated B-band absolute magnitude adopted by Hidalgo-Gámez & Olofsson rather than the uncertainty in the oxygen abundance. The position of Leo A with a new integrated B-band absolute magnitude (see next section) is shown in Fig. 2 by triangles (the positions of Leo A in the Z–L diagram with a new absolute magnitude and with absolute magnitude adopted by Hidalgo-Gámez & Olofsson are connected with a dashed line).

Thus, the determination of oxygen abundances in H II regions of low-luminosity irregular galaxies from the Hidalgo-Gámez & Olofsson sample with the P–method suggests that there is a well defined trend between M_B and O/H_P, and the large scatter in the low-luminosity end of the metallicity–luminosity relation obtained by Hidalgo-Gámez & Olofsson (1998) is explained mainly by the uncertainty in oxygen abundance determination with the T_e–method. In order to verify this conclusion, a larger sample of low-luminosity irregular galaxies will be considered in the next section.

2.3. The Z–L relationship of low-luminosity irregular galaxies

The data used in this study consists of published absolute magnitudes of irregular galaxies in B band and the intensities of [OII]$\lambda\lambda$3727, 3729 and [OIII]$\lambda\lambda$4959, 5007 emission lines. Our sample includes 34 data points in 20 irregular galaxies for which we have collected the relevant observational data, listed with references in Table 1. The commonly used name(s) of the galaxy are given in Cols. 1 and 2 and the label of the H II region or spectrum is given in Col. 3. The absolute blue magnitude M_B is listed in Col. 4 (references in Col. 5). The original oxygen abundance is given in Col. 6 (references in Col. 7). If the error range of the oxygen abundance determination was indicated by the author(s), this range is given in parentheses (Col. 6). If a method other than the T_e–method has been used for the oxygen abundance determination, this oxygen abundance is labeled with an asterisk.

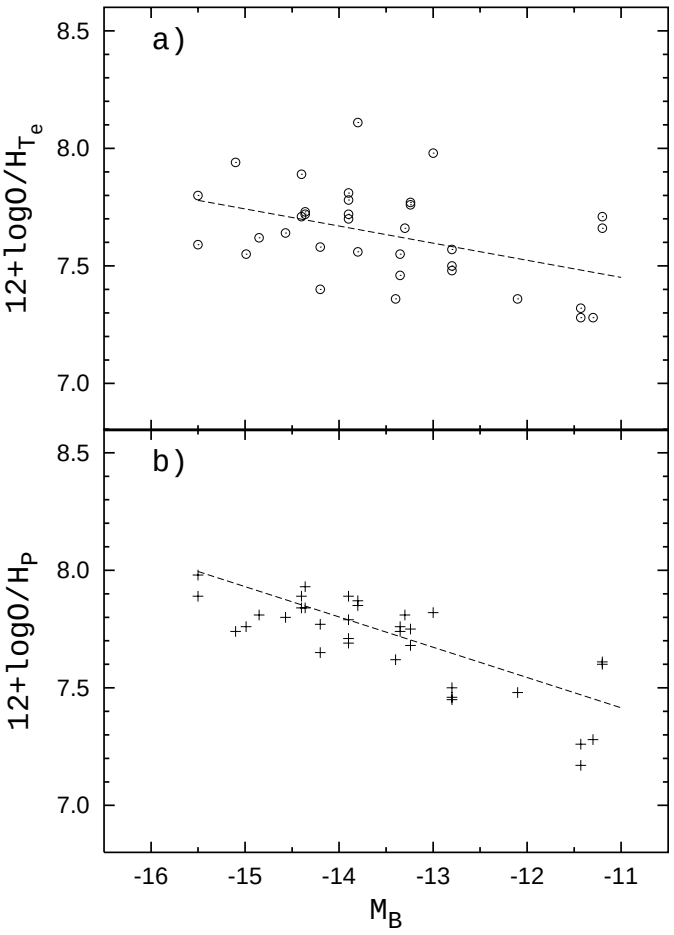

Fig. 3. The metallicity–luminosity diagram for dwarf irregular galaxies. The oxygen abundances for individual H II regions are shown. **a)** The L–Z diagram based on the oxygen abundances derived with the T_e–method or the empirical method (see Table 1). The line is the best fit. **b)** The L–Z diagram based on the oxygen abundances determined here with the P–method. The line is the best fit.

The oxygen abundances in H II regions have been calculated with the P–method using the published intensities (references in Col. 7) of [OII]$\lambda\lambda$3727, 3729 and [OIII]$\lambda\lambda$4959, 5007 emission lines. The derived oxygen abundances for individual H II regions are given in Col. 8 of Table 1. The metallicity–luminosity diagram for dwarf irregular galaxies based on the oxygen abundances derived here through the P–method is presented in Fig. 3 (panel *b*). The line is the best fit. For comparison, the metallicity–luminosity diagram for dwarf irregular galaxies based on the oxygen abundances derived through the T_e–method or empirical method (data from the Col. 6 of Table 1) is also presented in Fig. 3 (panel *a*). The line is the best fit.

Inspection of Fig. 3 shows that the metallicity–luminosity diagram for dwarf irregular galaxies based on

Table 1. Characteristics of the galaxies in the present sample.

galaxy	other name	H II region or spectrum label	M_B	reference	O/H[1]	reference	$(O/H)^1_P$ individual H II region	$(O/H)^1_P$ average for galaxy
Sextans B	DDO 70		−13.8	M	8.11	MAM	*7.87*	**7.86**
		No 2			7.56* (7.54–7.57)	SKH	*7.85*	
Sextans A	DDO 75	No 1	−14.2	M	7.40 (6.70–7.65)	SKH	*7.76*	**7.71**
		No 1h			7.58 (6.90–7.83)	SKH	*7.65*	
GR 8	DDO 155	H2a	−11.2	M	7.66	MAM	*7.61*	**7.60**
		H2b			7.71	MAM	*7.60*	
WLM	DDO 221	No 7	−13.9	M	7.72 (7.64–7.78)	HM	*7.71*	**7.78**
		No 9			7.81 (7.73–7.88)	HM	*7.69*	
		No 1			7.78 (7.48–7.95)	STM	*7.79*	
		No 2			7.70 (7.30–7.90)	STM	*7.89*	
UGC 4483		INT	−12.8	STKGT	7.50 (7.46–7.54)	STKGT	*7.45*	**7.47**
		McD			7.48 (7.42–7.54)	STKGT	*7.46*	
		WHT			7.57 (7.51–7.62)	STKGT	*7.50*	
Mkn 178		A	−14.36	H-GO	7.72	G-RRZ	*7.83*	**7.88**
		B			7.73	G-RRZ	*7.92*	
M81dB	UGC 5423		−12.9	MH94	7.98 (7.70–8.15)	MH	*7.81*	**7.81**
UGC 6456		Case 1	−13.24	RM	7.77	TBDS	*7.68*	**7.71**
		Case 2			7.76	TBDS	*7.75*	
Leo A	DDO 69		−11.3	M	7.28 (7.08–7.42)	SKH	*7.27*	**7.27**
DDO 187			−13.4	SKH	7.36* (7.23–7.46)	SKH	*7.62*	**7.62**
DDO 47		No 1	−14.4	H-GO	7.89 (7.64–8.05)	SKH	*7.84*	**7.86**
		No 3			7.71* (7.66–7.75)	SKH	*7.87*	
UGCA 292		No 1	−11.43	vZ	7.28 (7.23–7.33)	vZ	*7.26*	**7.22**
		No 2			7.32 (7.26–7.38)	vZ	*7.17*	
DDO 167			−13.3	SKH	7.66 (7.23–7.88)	SKH	*7.81*	**7.81**
SagDIG			−12.1	M	7.36*	STM	*7.48*	**7.48**
A1116+51			−14.99[2]	KD	7.55 (7.35–7.75)	KD	*7.76*	**7.76**
A1228+12			−14.57[2]	KD	7.64 (7.57–7.71)	KD	*7.79*	**7.79**
A2228-00			−14.85[2]	KD	7.62 (7.56–7.68)	KD	*7.81*	**7.81**
ESO 245-G05		19	−15.5	H-G99	7.80 (7.79–7.81)	H-G99	*7.98*	**7.94**
		12		H-G99	7.59 (7.57–7.61)	H-G99	*7.89*	
DDO 53		A	−13.35	H-G99	7.46 (7.39–7.53)	H-G99	*7.76*	**7.75**
		B		H-G99	7.55 (7.50–7.60)	H-G99	*7.74*	
DDO 190			−15.10	H-G99	7.94 (7.88–8.00)	H-G99	*7.74*	**7.74**

1 – In units of 12 + log(O/H).
2 – M_{pg} was taken as M_B.
*–Oxygen abundance was derived not through the T_e–method.

List of references to M_B:
H-G99 – Hidalgo-Gámez (1999); H-GO – Hidalgo-Gámez & Olofsson (1998); KD – Kinman & Davidson (1981); M – Mateo (1998); MH94 – Miller & Hodge (1994); RM – Richer & McCall (1995); SKH – Skillman et al. (1989); STKGT – Skillman et al. (1994); vZ – van Zee (2000)

List of references to oxygen abundances:
G-RRZ – González-Riestra et al. (1988); H-G99 – Hidalgo-Gámez (1999); HM – Hodge & Miller (1995); KD – Kinman & Davidson (1981); MAM – Moles et al. (1990); MH – Miller & Hodge (1996); SKH – Skillman et al. (1989); STKGT – Skillman et al. (1994); STM – Skillman et al. (1989); TBDS – Tully et al. (1981); vZ – van Zee (2000).

the oxygen abundances derived with the P–method shows relatively small scatter. It confirms the above conclusion that the large scatter in the low-luminosity end of the metallicity–luminosity relation for irregular galaxies obtained by Hidalgo-Gámez & Olofsson (1998) is explained mainly by the uncertainty in oxygen abundance determination with T_e–method.

The uncertainty in the integrated B-band absolute magnitudes M_B for irregular galaxies can also contribute to the dispersion in the Z–L diagram. The uncertainty in the distance determinations is the major source of uncertainty in the determination of the integrated B-band absolute magnitudes M_B for irregular galaxies. Therefore accurate distances to irregular galaxies are necessary in

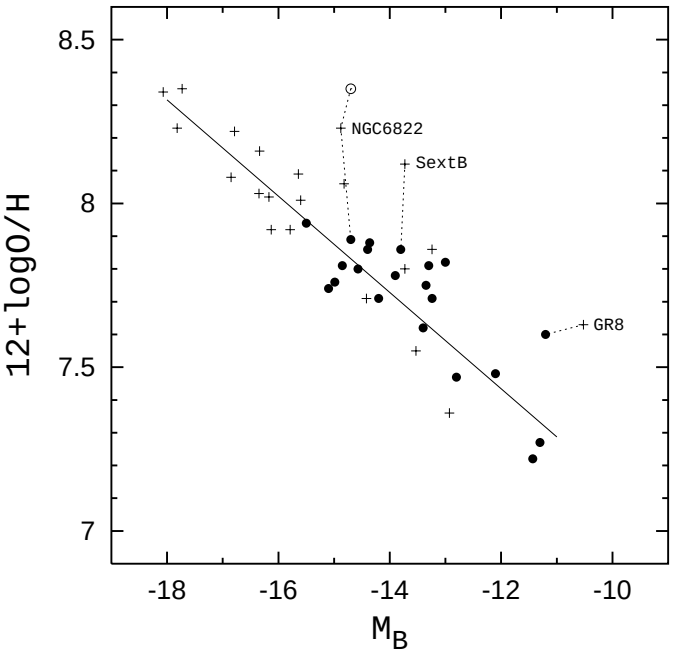

Fig. 4. The metallicity–luminosity diagram for dwarf irregular galaxies. The metallicity–luminosity diagram of Richer & McCall (1995) is represented by pluses. The metallicity–luminosity diagram based on the oxygen abundances derived with the P–method is shown by filled circles. The positions of Sextans B, GR8, and NGC 6822 with our data and their positions with Richer and McCall's data are connected by dashed lines. The open circle is the position of NGC 6822 with oxygen abundance from Eq. (4).

the construction of the Z–L diagram. Most galaxies considered here are members of the Local Group. The compilation of the recent information on distances for all the dwarf members and candidates of the Local Group is given by Mateo (1998). Nearly all of the members of the Local Group have reasonable distance determinations based on one or more high-precision distance indicator, including Cepheid variables. There are exceptions. In the case of Leo A there is a large discrepancy in the determined distances; Hoessel et al. (1994) found a value of 2.2 Mpc on the basis of Cepheid variables. More recently, Tolstoy et al. (1998) (based on the position of the red clump, the helium-burning blue loops, and the tip of the red giant branch) obtained the value of 690 ± 60 kpc. The short distance resolves the problems which appear for Leo A in the case of long distance, (see discussion in Mateo 1998, and references therein). The short distance makes the position of Leo A much closer to the metallicity–luminosity relationship (see Fig. 2).

The comparison of our Z–L diagram with that of Richer & McCall (1995) is given in Fig. 4. The pluses are data of Richer & McCall (1995), the filled circles are the data for irregular galaxies from the present sample. The oxygen abundances $\mathrm{O/H}_P$ used in the construction of the Z–L diagram in Fig. 4 are the values obtained by averaging all the available determinations for a given galaxy (Col. 9 in Table 1). The solid line is the metallicity–luminosity relationship obtained by Richer & McCall (1995) for the luminous ($M_B < -15$) irregular galaxies. As can be seen in Fig. 4, the metallicity–luminosity relation for low-luminosity dwarf irregular galaxies derived here is in good agreement with the metallicity–luminosity relation obtained by Richer & McCall (1995). However, the positions of some galaxies in our metallicity–luminosity diagram and in the diagram of Richer & McCall are appreciable different.

According to the data of Richer & McCall the positions of three galaxies (Sextans B, GR8, and NGC 6822) in the Z–L diagram have large deviations from the metallicity–luminosity relationship (Fig. 4). The positions of Sextans B and GR8 in the Z–L diagram with our data show significantly smaller deviations from the metallicity–luminosity relationship than their positions with Richer and McCall's data. (The positions of Sextans B, GR8, and NGC 6822 in the Z–L diagram with our data and positions with Richer and McCall's data are connected with dashed lines in Fig. 4.) There are two determinations of oxygen abundance in Sextans B (Table 1) which result in different values of oxygen abundance: $12 + \log \mathrm{O/H} = 7.56$ according to Skillman et al. (1989a) and $12 + \log \mathrm{O/H} = 8.11$ according to Moles et al. (1990). The value of oxygen abundances from Moles et al. (1990) has been adopted by Richer & McCall (1995). The oxygen abundances derived through the P–method with the line intensities measurements from Skillman et al. (1989a) and from Moles et al. (1990) are in good argeement: $12 + \log \mathrm{O/H} = 7.85$ for the Skillman et al.'s data and $12 + \log \mathrm{O/H} = 7.87$ for the Moles et al.'s data (Table 1). This value of oxygen abundance in the Sextans B is in agreement with oxygen abundance corresponding to its luminosity according to the metallicity–luminosity relationship. A large deviation of the position of GR8 in the Richer and McCall Z–L diagram from the metallicity–luminosity relationship is caused mainly by the uncertainty in the value of the luminosity, Fig. 4. The case of NGC 6822 will be considered in the next subsection.

Thus, the metallicity–luminosity diagram for low-luminosity dwarf irregular galaxies constructed here on the base of oxygen abundances derived through the P–method is in good agreement with the metallicity–luminosity relation obtained by Richer & McCall (1995). It should be particularly emphasized that Richer & McCall have determined their metallicity–luminosity relation using only the best available data for dwarf irregulars. In contrast, we have constructed the metallicity–luminosity diagram using all the available data for dwarf irregulars. As a consequance of this, the number of points at the low-luminosity end of the metallicity–luminosity relation increases by about a factor of two. As this takes place, the scatter at low luminosities in our diagram is not in excess of that in Richer and McCall's diagram, although the dispersion of oxygen abundances around the metallicity–luminosity relationship seems to increase with decreasing galaxy luminosity, as was found by Richer & McCall (1995).

Table 2. Oxygen abundances in H II regions of the dwarf irregular galaxy NGC 6822. The name of the H II region is reported in Col. 1. The original oxygen abundance is reported in Col. 2 (reference in Col. 3). The oxygen abundance derived through the T_e–method is labeled "Te". The oxygen abundance derived here through the P–method is listed in Col. 4.

H II region	12+log O/H	reference	12+log $(O/H)_P$
Ho 11	8.24 ± 0.20	Petal	8.25
Ho 12	8.23 ± 0.20	Petal	8.32
Hu X	8.21 ± 0.15 (Te)	Petal	8.44
Hu V	8.20 ± 0.09 (Te)	Petal	8.40
Ho 14	8.27 ± 0.20	Petal	(8.01)
Ho 13	8.50 ± 0.20	Petal	8.32
Ho 15	8.11 ± 0.12 (Te)	Petal	8.31
Hu X	8.27 ± 0.06 (Te)	Letal	8.34
Hu V	8.20 ± 0.06 (Te)	Letal	8.38
Hu V	8.20 ± 0.12	STM	8.37
Hu V	8.13 ± 0.02 (Te)	H-G	8.38
Hu X	8.09 ± 0.06 (Te)	H-G	8.34
mean	8.23		8.35

List of references:
H-G – Hidalgo-Gámez (1999); Letal – Lequeux et al. (1979); Petal – Pagel et al. (1980); STM – Skillman et al. (1989)

2.4. The NGC 6822

The position of NGC 6822 in the Z–L diagram shows a large deviation from the metallicity–luminosity relationship (Fig. 4). The oxygen abundance determinations both in individual stars and in H II regions in the NGC 6822 are now available. The mean stellar oxygen abundance derived from high resolution spectra of two stars is $12 + \log \mathrm{O/H_{star}} = 8.36 \pm 0.19$ (Venn et al. 2001). Twelve determinations of oxygen abundances in H II regions of the NGC 6822 (Lequeux et al. 1979; Pagel et al. 1980; Skillman et al. 1989b; Hidalgo-Gámez 1999) result in a mean value of gas oxygen abundance $12 + \log \mathrm{O/H} = 8.23$ (Table 2). If this value of gas oxygen abundance in the NGC 6822 is correct, then the position of NGC 6822 in the metallicity–luminosity diagram deviates considerably from the metallicity–luminosity relationship, i.e. this value of oxygen abundance in the NGC 6822 is significantly (by around 0.3 dex) higher than the oxygen abundance corresponding to its luminosity, Fig. 4.

If H II regions in NGC 6822 lie on the lower branch of the R_{23}–O/H diagram then, Eq. (3) can be used for the oxygen abundance determination in H II regions of NGC 6822. The mean value of oxygen abundances obtained via Eq. (3) is around 7.90. In this case the position of the NGC 6822 in the Z–L diagram is close to the metallicity–luminosity relationship, Fig. 4, but this value of oxygen abundance is in conflict with a stellar oxygen abundance 12+log $\mathrm{O/H_{star}}$ and with the oxygen abundances of $\mathrm{O/H}_{T_e}$ derived through the T_e–method (Table 2).

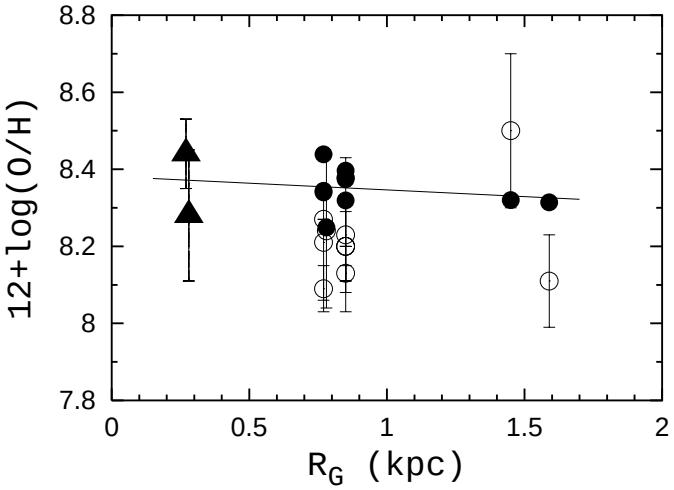

Fig. 5. The radial abundance gradient within NGC 6822. The original oxygen abundances of H II regions (Col. 2 of Table 2) are represented by open circles with error bars. The stellar data (with error bars) are shown by filled triangles. Our oxygen abundances $\mathrm{O/H}_P$ for H II regions (Col. 4 of Table 2) are shown by filled circles. The line is the best fit to our data for H II regions and to the original data for stars.

The stellar oxygen abundances and oxygen abundances derived through the T_e–method suggest that the H II regions in NGC 6822 lie on the upper branch of the R_{23}–O/H diagram. Then, the corresponding equation from Paper II

$$12 + \log(\mathrm{O/H})_P = \frac{R_{23} + 54.2 + 59.45P + 7.31P^2}{6.07 + 6.71P + 0.371P^2 + 0.243R_{23}} \quad (4)$$

should be used for the oxygen abundance determination in H II regions of NGC 6822. In this case the mean oxygen abundance for 11 H II regions in NGC 6822 is $12 + \log \mathrm{O/H}_P = 8.35$, Table 2 (the value of $\mathrm{O/H}_P$ obtained in the H II region Ho 14 from the sample of Pagel et al. (1980) is in conflict with the suggestion that this H II region belongs to the upper branch of the R_{23}–O/H diagram, and this H II region is excluded from the consideration). The mean value of $\mathrm{O/H}_P$ is in agreement with the mean value of the stellar oxygen abundance. But in this case the position of the NGC 6822 in the Z–L diagram deviates considerably from the metallicity–luminosity relationship (open circle in Fig. 4).

The values of the distance modulus of NGC 6822 determined with different distance indicators (Cepheids, the tip of the red giant branch) are in good agreement (Lee et al. 1993; Gallart et al. 1996; Ferrarese et al. 2000); the uncertainty seems to be not in excess of ± 0.15. Therefore the deviation of NGC 6822 from the metallicity–luminosity relation cannot be caused by the uncertainty in the luminosity determination. Thus, the large deviation of NGC 6822 from the metallicity–luminosity relationship seems to be real, although the actual value of the deviation is not clear.

In Fig. 5 we show our oxygen abundances $\mathrm{O/H}_P$ for H II regions from Table 2, as a function of galactocentric distance, together with the original oxygen abundances in

H II regions and with data for stars. The original oxygen abundances are presented by open circles with error bars. The stellar data (with error bars) are shown by filled triangles. Our data are shown with filled circles. The galactocentric distances for H II regions and stars were taken from Venn et al. (2001). The line is the best fit to our data for H II regions and to the original data for stars. From examination of the O/H_P in the H II regions together with the stellar data, it is evident that there is no significant radial abundance gradient within the NGC 6822. The slope of the formal best fit is about -0.035 dex/kpc. The data are also consistent with no gradient at all. Thus, our data confirm the conclusion of Pagel et al. (1980) that if there is an actual radial abundance gradient within NGC 6822, the slope of the gradient is small and the trend is entirely masked by the errors.

3. Discussion and conclusions

Thus, the metallicity–luminosity relation for irregular galaxies extends into the region of low luminosities up to $M_B \sim -12$. It is widely suggested that the metallicity–luminosity relation for irregular galaxies is caused by galactic winds of different efficiencies. In other words, the metallicity–luminosity relation represents the ability of a given galaxy to keep the products of its own evolution rather than their ability to produce metals (Larson 1974). On the other hand, it has been found that the astration level is higher in massive irregular galaxies than in dwarf ones (Lequeux et al. 1979; Vigroux et al. 1987). Then, it is suggested that the systematic increase of the astration level with luminosity can aslo play a role in the origin of the metallicity–luminosity relationship for irregular galaxies.

The values of the gas mass fraction μ and oxygen abundance deficiency (which is a good indicator of the efficiency of mass exchange between a galaxy and its environment) have been derived for a number of late-type spiral (Pilyugin & Ferrini 1998) and irregular (Pilyugin & Ferrini 2000a) galaxies. Using these data, the roles of two hypothesed mechanisms as causes of the metallicity–luminosity correlation among late-type spiral and irregular galaxies have been examined in our recent study (Pilyugin & Ferrini 2000b). It was found that both the increase in astration level and the decreasing efficiency of heavy element loss with increasing luminosity, make comparable contributions to the metallicity–luminosity correlation. The fact that the metallicity–luminosity relation for irregular galaxies extends up to low luminosity can be considered as evidence that the tendency for the decrease in astration level and the increasing efficiency of heavy element loss with decreasing luminosity remains at the low-luminosity end.

A prominent feature of the metallicity–luminosity relation for irregular galaxies is the increased scatter at low luminosities in comparison to that at high luminosities. Part of this scatter is undoubtedly due to uncertainties in the oxygen abundances and luminosities. But another part is likely to be real. Since there is no apparent reason to suggest that the uncertainties in oxygen abundances and/or in luminosities increase systematically with decreasing galaxy luminosity, the increase of the dispersion of oxygen abundances around the metallicity–luminosity relationship with decreasing galaxy luminosity seems to be real. The increase in the scatter of oxygen abundances with luminosity can be explained by the fluctuations in values of the gas mass fraction among irregular galaxies of a given luminosity. There is a correlation between the gas mass fraction μ and the galaxy's luminosity, decreasing from $\mu \sim 0.8$ at $M_B = -12$ or $\log L_B = 7$ to $\mu \sim 0.4$ at $M_B = -18$ or $\log L_B = 9.4$ (Pilyugin & Ferrini 2000a). According to the simple model for the chemical evolution of galaxies, the relation between oxygen abundance and gas mass fraction is given by a logarithmic relationship, $Z_O \sim \ln(1/\mu)$, then the O/H–μ curve is significantly steeper at large than at small μ. Therefore, the equal fluctuations in values of the gas mass fraction, say $\Delta\mu = 0.1$, result in an appreciably larger dispersion of oxygen abundances among low-luminosity irregular galaxies with high values of the gas mass fraction (the change of μ from 0.9 to 0.8 results in $\Delta \log O/H \sim 0.33$) than among luminous irregular galaxies with low values of the gas mass fraction (the change of μ from 0.5 to 0.4 results in $\Delta \log O/H \sim 0.12$). Thus, the increase in the scatter of oxygen abundances with luminosity is not surprising.

In summary:

The low-luminosity dwarf irregular galaxies are considered. The oxygen abundances in H II regions of dwarf irregular galaxies were recalculated from published spectra through the recently suggested P–method. It has been found that the metallicity of low-luminosity dwarf irregular galaxies, with a few exceptions, correlates well with galaxy luminosity. The dispersion of oxygen abundances around the luminosity–metallicity relationship increases with decreasing galaxy luminosity, as was found by Richer & McCall (1995). The lack of relationship between the oxygen abundance and the absolute magnitude in the blue band for irregular galaxies obtained by Hidalgo-Gámez & Olofsson (1998) can be explained by the large uncertainties in the oxygen abundances derived through the T_e–method, that in turn can be explained by the large uncertainties in the measurements of the strengths of the weak oxygen line [OIII]λ4363 used in the T_e–method.

Acknowledgements. It is a pleasure to thank the referee, Dr. N. Arimoto, for his comments on this work. This study was partly supported by the NATO grant PST.CLG.976036 and the Joint Research Project between Eastern Europe and Switzerland (SCOPE) No. 7UKPJ62178.

References

Ferrarese, L., Mould, J. R., Kennicutt, R. C., et al. 2000, ApJ, 529, 745

Gallart, C., Aparicio, A., & Vilchez, J. M. 1996, AJ, 112, 1928

Garnett, D. R., & Shields, G. A. 1987, ApJ, 317, 82

Garnett, D. R., Shields, G. A., Skillman, E. D., Sagan, S. P., & Dufour, R. J. 1997, ApJ, 489, 63
González-Riestra, R., Rego, M., & Zamorano, J. 1988, A&A, 202, 27
Heydari-Malayeri, M., Melnick, J., & Martin, J.-M. 1990, A&A, 234, 99
Hidalgo-Gámez, A. M. 1999, Dissertation for the Degree of Doctor of Philosophy in Astronomy, Uppsala University
Hidalgo-Gámez, A. M., & Olofsson, K. 1998, A&A, 334, 45
Hodge, P., & Miller, B. W. 1995, ApJ, 451, 176
Hoessel, J. G., Saha, A., Krist, J., & Danielson, G. E. 1998, AJ, 108, 645
Hunter, D. A., & Hoffman, L. 2000, AJ, 117, 2789
Izotov, Y. I., & Thuan, T. X. 1999, ApJ, 511, 639
Larson, R. B. 1974, MNRAS, 169, 229
Lee, M. G., Freedman, W. L., & Madore, B. F. 1993, ApJ, 417, 553
Lequeux, J., Peimbert, M., Rayo, J. F., Serrano, A., & Torres-Peimbert, S. 1979, A&A, 80, 155
Kinman, T. D., & Davidson, K. 1981, ApJ, 243, 127
Mateo, M. 1998, ARA&A, 36, 435
McGaugh, S. S. 1991, ApJ, 380, 140
Miller, B. W., & Hodge, P. 1994, ApJ, 427, 656
Miller, B. W., & Hodge, P. 1996, ApJ, 458, 467
Moles, M., Aparicio, A., & Masegosa, J. 1990, A&A, 228, 310
Pagel, B. E. J., Edmunds, M. G., & Smith, G. 1980, MNRAS, 193, 219
Pilyugin, L. S. 2000, A&A, 362, 325 (Paper I)
Pilyugin, L. S. 2001, A&A, 369, 594 (Paper II)
Pilyugin, L. S., & Ferrini, F. 1998, A&A, 336, 103
Pilyugin, L. S., & Ferrini, F. 2000a, A&A, 354, 874
Pilyugin, L. S., & Ferrini, F. 2000b, A&A, 358, 72
Richer, M. G., & McCall, M. L. 1995, ApJ, 445, 642
Skillman, E. D., Kennicutt, R. C., & Hodge, P. W. 1989a, ApJ, 347, 875
Skillman, E. D., Terlevich, R., Kennicutt, R. C., Garnett, D. R., & Terlevich, E. 1994, ApJ, 431, 172
Skillman, E. D., Terlevich, R., & Melnick, J. 1989b, MNRAS, 240, 563
Tolstoy, E., Gallagher, J. S., Cole, A. A., et al. 1998, AJ, 116, 1244
Tully, R. B., Boesgaard, A. M., Dyck, H. M., & Schempp, W. V. 1981, ApJ, 246, 38
van Zee, L. 2000, ApJL, 543, 31L
Venn, K. A., Lennon, D. J., Kaufer, A., et al. 2001, ApJ, 547, 765
Vigroux, L., Stasinska, G., & Comte, G. 1987, A&A, 172, 15
Vila-Costas, M. B., & Edmunds, M. G. 1992, MNRAS, 259, 121
Webster, B. L., Longmore, A. J., Hawarden, T. G., & Mebold, U. 1983, MNRAS, 205, 643
Zaritsky, D., Kennicutt, R. C., & Huchra, J. P. 1994, ApJ, 420, 87